NATURAL SMALL ELMS ACHIEVED AT LOW PEDESTAL COLLISIONALITY (<1) IN A METAL WALL ENVIRONMENT ON EAST

Yifeng Wang[1], Huiqian Wang[2], Xueqiao Xu[3], Guosheng Xu[1], Nami Li[3], Qingquan Yang[1], Xin Lin[1], Qing Zang[1], Tao Zhang[1], Yifei Jin[1], Minrui Wang[1], Guozhang Jia[1], Ning Yan[1], Ran Chen[1], Liang Wang[1] and EAST Team

[1]Institute of Plasma Physics, Chinese Academy of Sciences, Hefei, China
[2]General Atomics, San Diego, USA
[3]Lawrence Livermore National Laboratory, Livermore, USA

Email: yfwang@ipp.ac.cn

Low pedestal collisionality with high auxiliary heating power is anticipated in future fusion reactors. How to avoid transient heat load induced by large-amplitude edge-localized modes (ELMs) at low pedestal collisionality without significant degradation of the plasma performance is one of critical issues for achieving stationary high-confinement mode (H-mode) operation of the next-step tokamak fusion reactors. The grassy ELM regime with intrinsic small-amplitude ELMs and good energy confinement has been found to be compatible with low pedestal collisionality. A detailed physics understanding of the access to this regime at low pedestal collisionality is critical to realize the grassy ELM regime in future fusion reactors, such as ITER and CFETR.

In this work, we report small ELMs achieved at low pedestal collisionality ($\nu^*_{e,ped}$<1) with high heating power and low plasma density on EAST. Fig. 1 shows time traces for two discharges #114651 (blue) and #114655 (red) on EAST. Small ELMs (f_{ELM}~600Hz) are achieved in #114651 in near double null (near-DN) configuration with dR_{sep}~ 5 mm, while ELMs (f_{ELM}~200Hz) are much larger in #114655 in lower single null (LSN) configuration with dR_{sep}~ -20 mm. Both discharges have similar plasma parameters, such as plasma current I_p ~ 450 kA, toroidal magnetic field B_t ~ 2.3 T, plasma line-averaged electron density $\bar{n}_e$ ~ 3.1×10^{19} m^{-3} at about 3 s, internal inductance l_i ~ 1.0, plasma total stored energy W_{MHD} ~ 210 kJ and total heating power. The heating power consists of 1.0 MW 4.6 GHz LHW, 1.45 MW ECRH and 5.2 MW NBI in both discharges. During the discharge #114651, gas fueling has been turned off from 3 s and then plasma density decreases from 3.1 to 2.8×10^{19} m^{-3}. The ELM frequency appears to decrease as density increases. This is similar with the ELM behavior observed in discharge #114655, where the ELM frequency increases during the density ramp-up process. In addition, the ELM behavior at low pedestal collisionality appears to be obviously dependent on the plasma configuration. As shown in Fig. 1, the near-DN configuration appears to facilitate the access to the small ELM regime. Based on the measured electron density and temperature profiles, the equilibria of both the large ELMs and small ELMs cases are reconstructed with the kinetic EFIT code and the pedestal peeling-ballooning mode (PBM) stability has been analyzed with the ELITE code as shown in Fig. 2. Linear pedestal stability analysis suggests that the ballooning stability boundary significantly expands with the DN configuration, making the operational point move away from the corner of the PBM instability boundary, where peeling modes and ballooning modes are thought to be strongly coupled and type-I ELMs are more likely to be triggered. To further confirm the effect of plasma configuration on the ELM instability, the plasma configurations are exchanged numerically in #114651 and #114655 and the corresponding equilibria are recalculated. As shown in Fig. 3 (a)(b), the red dashed lines represent edge profiles in the new equilibrium of #114655 with plasma configuration of #114651 and the blue dashed lines represent edge profiles in the new equilibrium of #114651 with plasma configuration of #114655. The pedestal PBM stability of

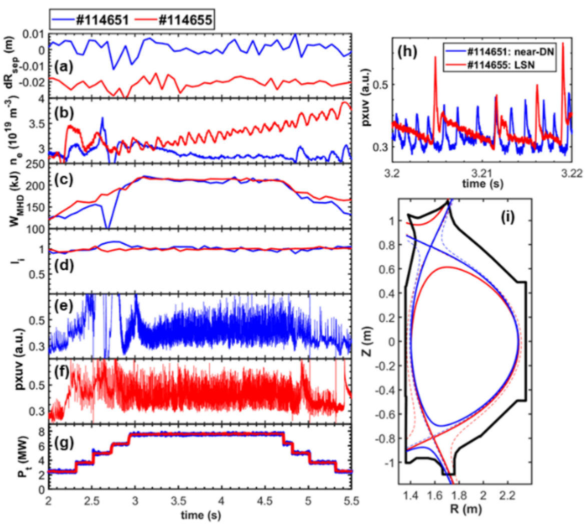

FIG. 1. Small ELMs (f_{ELM}~600Hz, blue) have been achieved at low pedestal collisionality (<1) with near double null configuration, in comparison with larger ELMs (f_{ELM}~200Hz, red) achieved with lower single null configuration on EAST. (a) dR_{sep}, (b) plasma line-averaged density $\bar{n}_e$, (c) plasma stored energy W_{MHD}, (d) internal inductance l_i, XUV signals in (e) #114651 and (f) #114655, (g) total heating power P_t, (h) enlarged view of the XUV signals and (i) plasma configurations are shown.

the new equilibrium of #114655 with plasma configuration of #114651 are analyzed with the ELITE code as shown in Fig. 3 (c) (red dashed line and hollow circle). As shown in Fig. 3, with near-DN configuration of #114651, the pressure pedestal of the red dashed case becomes steeper than the red solid case, as well as a higher peak current density. The plasma configuration would also affect the weighting of magnetic field lines in the outboard bad curvature region. As a result, the ballooning instability boundary expands, making the operational point away from the corner of the PBM instability boundary.

We have also investigated the effect of strike point location on the access to the small ELM regime at low pedestal collisionality on EAST. Under the conditions of high plasma density and low heating power, large ELMs have been successfully mitigated by changing strike point location on the divertor target plate, accompanied by significantly enhanced separatrix density. This is correlated with a higher ionization source in scrape-off layer region when the strike point moves away from the divertor corner region, which is thought to provide a strong fuelling near separatrix and thus enhance the separatrix density. Linear pedestal stability analysis suggests that the operational point is located near the ballooning stability boundary. However, under the conditions of low plasma density and high heating power, large ELMs are not mitigated by changing strike point location. The separatrix density appears to be nearly unchanged, which is thought to be due to the low edge fuel recycling under these conditions. Further work is needed to find key plasma parameters for access to the small ELM regime at low pedestal collisionality and to better understand the physical mechanism behind.

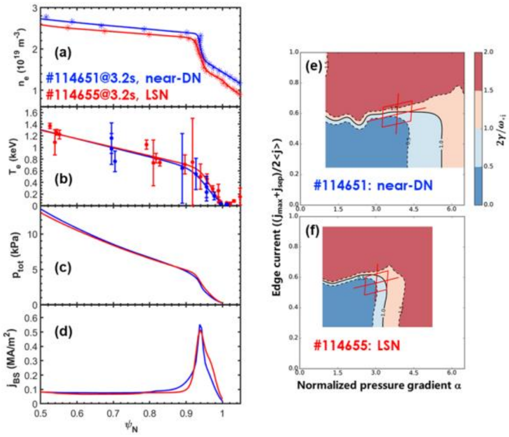

FIG. 2. Comparison of edge profiles of (a) electron density, (b) electron temperature, (c) total pressure and (d) bootstrap current density and (e)(f) pedestal PBM stability diagrams between #114651 (blue) in the small ELM phase and #114655 (red) in the large ELM phase are shown.

ACKNOWLEDGEMENTS

This work was supported by the National Magnetic Confinement Fusion Energy Program of China under Grant No. 2019YFE03030000 and the National Natural Science Foundation of China under Contract Nos. 12005263.

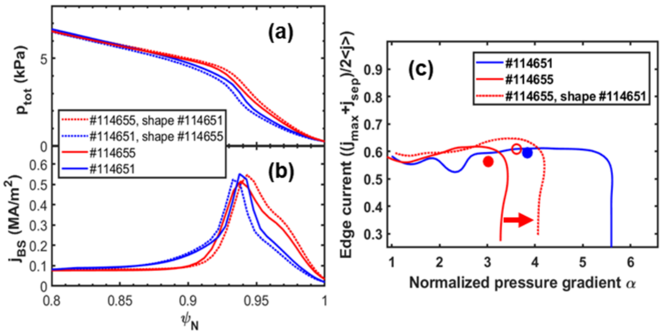

FIG. 3. The plasma shapes in #114651 and #114655 are exchanged numerically and the equilibria are recalculated. The edge profiles of (a) pressure and (b) bootstrap current of the recalculated equilibria (dotted lines) are shown as well as the PBM stability diagram for the new equilibrium of #114655 with plasma shape from #114651 (red dashed line and hollow circle) in (c).

REFERENCES

[1] WANG, Y.F., et al., “Grassy ELM regime at low pedestal collisionality in high-power tokamak plasma”, Nucl. Fusion 61 016032 (2021).

[2] ZHANG, H., et al., “Observation of a fully non-inductive H-mode regime dominated by the sporadic-small edge-localized modes in EAST with a tungsten divertor”, Plasma Phys. Control. Fusion 61 085006 (2019).

[3] WANG, Y.F., et al., “Dependence of ELM instability on separatrix density in EAST long-pulse H-mode plasmas”, Nucl. Fusion 64 126017 (2024).